Conoscopic Holography for Image Registration: A Feasibility Study

Ray A. Lathrop*, Tiffany T. Cheng, and Robert J. Webster III
Dept. of Mechanical Engineering, Vanderbilt University, Nashville, TN USA 37235

ABSTRACT

Preoperative image data can facilitate intrasurgical guidance by revealing interior features of opaque tissues, provided image data can be accurately registered to the physical patient. Registration is challenging in organs that are deformable and lack features suitable for use as alignment fiducials (e.g. liver, kidneys, etc.). However, provided intraoperative sensing of surface contours can be accomplished, a variety of rigid and deformable 3D surface registration techniques become applicable. In this paper, we evaluate the feasibility of conoscopic holography as a new method to sense organ surface shape. We also describe potential advantages of conoscopic holography, including the promise of replacing open surgery with a laparoscopic approach. Our feasibility study investigated use of a tracked off-the-shelf conoscopic holography unit to perform a surface scans on several types of biological and synthetic phantom tissues. After first exploring baseline accuracy and repeatability of distance measurements, we performed a number of surface scan experiments on the phantom and ex vivo tissues with a variety of surface properties and shapes. These indicate that conoscopic holography is capable of generating surface point clouds of at least comparable (and perhaps eventually improved) accuracy in comparison to published experimental laser triangulation-based surface scanning results.

Keywords: Registration, Surface Scan, Liver, Robot, Image-Guided Surgery, Conoscope, Medical Holography

1. INTRODUCTION

The purpose of our study is to investigate the feasibility of conoscopic holography as a sensing system for organ surface contours – that is, for obtaining a point cloud that describes the surface. Conoscopic holography is sensing strategy employed in some inspection profilometers, devices used in industry to make highly accurate and precise measurements of machine components. While in principle a conoscopic holography has the potential to act as a camera that provides 3D distance measurements to any point in the image it captures, this promise has not yet been realized. This is due to the highly challenging computational and algorithmic issues involved with converting raw data (Fresnel patterns) to distances in the 3D case. However, in the simpler case of collecting 1D distance measurements axially outward from the lens, the technology is mature and measurements are highly precise. Current commercial implementations shine a laser "dot" at the measurement site, and determine the linear distance to it by observing reflected light. In the surgical setting, conoscopic holography promises not only accurate surface scanning, but also scanning through a laparoscopic port. This has the potential to reduce invasiveness by eliminating the need for the open surgery often required by current probe and laser triangulation-based organ contour sensing techniques.

1.1 Background

A number of strategies have been have been successfully employed to register the surface of a body part or organ to preoperative scans (e.g. computer aided tomography or magnetic resonance images). Surface-based image registration is generally required for procedures where fiducial-based registration is infeasible due to location, tissue deformation, or other factors. Surfaced-based registration requires sensing a large number of points that describe the surface contour, combined with an algorithm for aligning the sensed surface with segmented preoperative image data [1,2].

Several probe-based methods for acquiring a set of points describing the organ surface have been investigated, including interaoperative ultrasound (US), as well as optically or magnetically tracked touch-probes. Intraoperative ultrasound senses subsurface features in slices, which can be advantageous in comparison to purely surface information. However, it can be challenging to deploy and use US minimally invasively (e.g. laparoscopically), and US by its nature requires direct tissue contact which may deform the organ or obscure the surface, limiting the access of other tools. Another option is an optically or magnetically tracked mechanical probe. With such a probe, liver surface scanning has been accomplished with surface scan errors of 2.9mm RMS, in comparison to a rigidly registered point cloud describing the

*ray.a.lathrop@vanderbilt.edu phone 1 615 322-0193; fax 1 615 343-6687; http://research.vuse.vanderbilt.edu/MEDLab/

same surface [3]. However, similarly to US, optically and magnetically tracked probes require tissue surface contact, implying that variations in pressure may cause measurement errors, and there is risk of tissue irritation or damage from probe contact.

A non-contact option is triangulation-based laser range finding, which has been FDA approved for abdominal use [1,4,5]. These devices have demonstrated clinical usefulness and commercial viability, but current laser range scanners require wide organ exposure, which precludes their use in laparoscopic procedures and motivates our work. We note that independent of the method used to collect surface data, registration may be accomplished with a variety of methods including Horn's quaternion method, the iterative closest point algorithm, etc. (see e.g. [1,5]).

1.2 Conoscopic Holography Overview

We propose conoscopic holography as an alternative to probe-based or laser triangulation-based systems for collecting point clouds describing organ surfaces. Conoscopic holography is based on polarized light interference inside of a birefringent crystal [6,7]. Figure 1 shows an Optimet Conoprobe sensor with a conceptual diagram of the basic components generally used in conoscopic holography overlaid. During a measurement, the target point is illuminated with a columnated light source such as a laser that has been emitted by a laser diode and then projected along the outward optical path via a beam splitter. The uncolumnated reflected light returning to the conoscope passes through a polarizing filter and then a birefringent crystal which generates an interference pattern [6]. The pattern is projected through a second polarizing filter and then recorded using a Charge Coupled Device (CCD) sensor. Distance measurements can be extracted from the resulting Fresnel zone pattern.

1.3 Application of Conoscopic Holography to Surface Scanning

To create a laparoscopic surface scan with conoscopic holography, we envision a system like the one shown in Figure 2. Here, the conoscope is fixed to one end of a hollow tube, which passes through a standard laparoscopic port. The conoscope is tracked using an optical or magnetic tracking system or with a mechanical encoding arm, and provides distance measurements to points on tissue. As the laser dot is moved over the organ surface by appropriate manual manipulation of the conoscope, it will produce a cloud of surface points on the organ, to which preoperative image data can be registered. We note that it is possible to use a mirror to redirect the conoscope beam, and that an eventual commercial system may not require manual manipulation in order to trace out the surface contour with the laser beam.

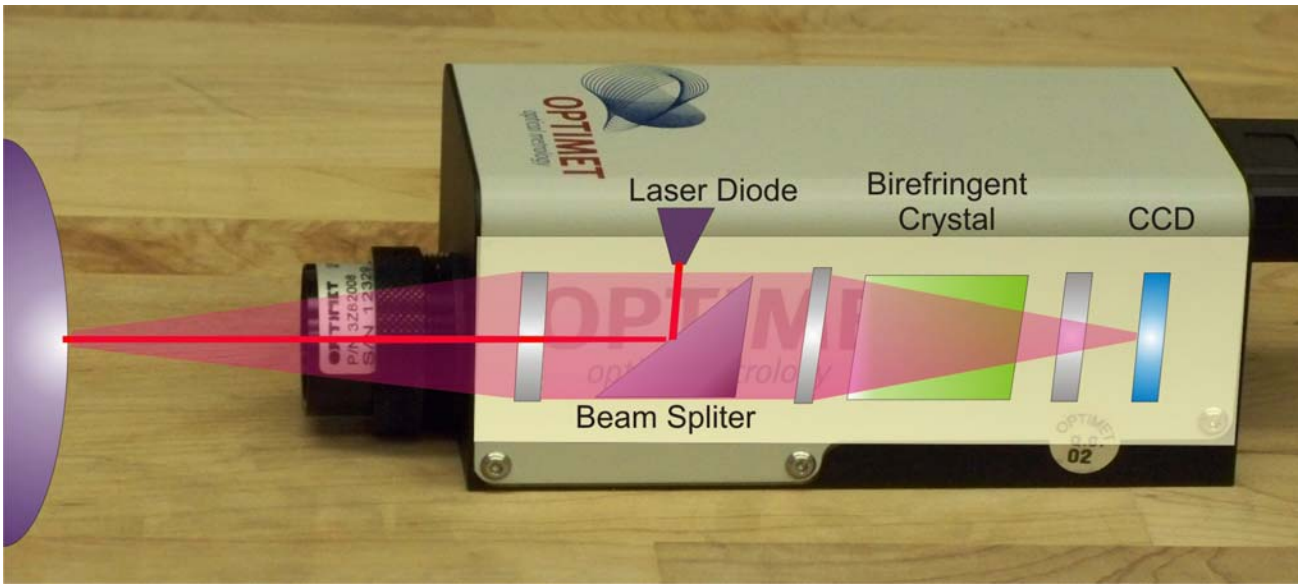

Figure 1. A photograph of the Optimet Conoprobe Mark 3.0, the off-the-shelf conoscopic holography system used in our experiments, which provides highly precise 1D distance measurements. Superimposed is a conceptual diagram of the basic components generally used in conoscopic holography, which process the returned light. The end product is an interference fringe pattern on the CCD sensing array at the back of the device, from which distances are computed.

2. EXPERIMENTAL TESTBED

We conducted a series of experiments as described in Sections 3 and 4 to assess the feasibility of applying conoscopic holography for registration of point clouds to known surfaces. These experiments consist of a basic repeatability and accuracy study to assess the conoscope's ability to collect data from biological tissue surfaces, as well as several surface scanning experiments. Before discussing these experiments, we first describe the overall experimental setup, which consists of the conoscope, a robotic arm, an optical tracking system, and the synthetic and biological phantoms used in experiments.

2.1 Conoscope

Precision. As mentioned earlier, in this paper we use the Conoprobe Mark 3 (Optimet, Inc.). The device's published specifications with a 200mm lens list a measurement precision of <70µm. The lateral size of the laser measurement spot is 170µm. Specifications for the 250mm lens used in our experiments are not published, but are similar. It is also known that surfaces which diffuse the red laser light of the scanner can reduce accuracy of the measurement, which motivates our experiments in Section 3 to validate the precision of the conoscope under these conditions.

Suitability for laparoscopy. The measurement range of the conoscope depends on the focal length of its lens. With a 250mm lens the range is 155-337mm, which is reasonable for use in laparoscopic surgery. Since light returns from the measurement spot to the conoscope in a conical shape (see Figure 2), one must also ensure[1] that the 10mm trocar will not interfere with the beam. Using the inside diameter of the lens barrel (22.8mm) for the base of the cone, the return beam will be 10mm wide at 44% of its return path. Thus, the distance between the trocar and the desired measurement point (see Figure 2), must be 0-148mm for our particular lens, which has a maximum working distance of 337mm. We note that these values can be designed as desired by choosing the appropriate lens.

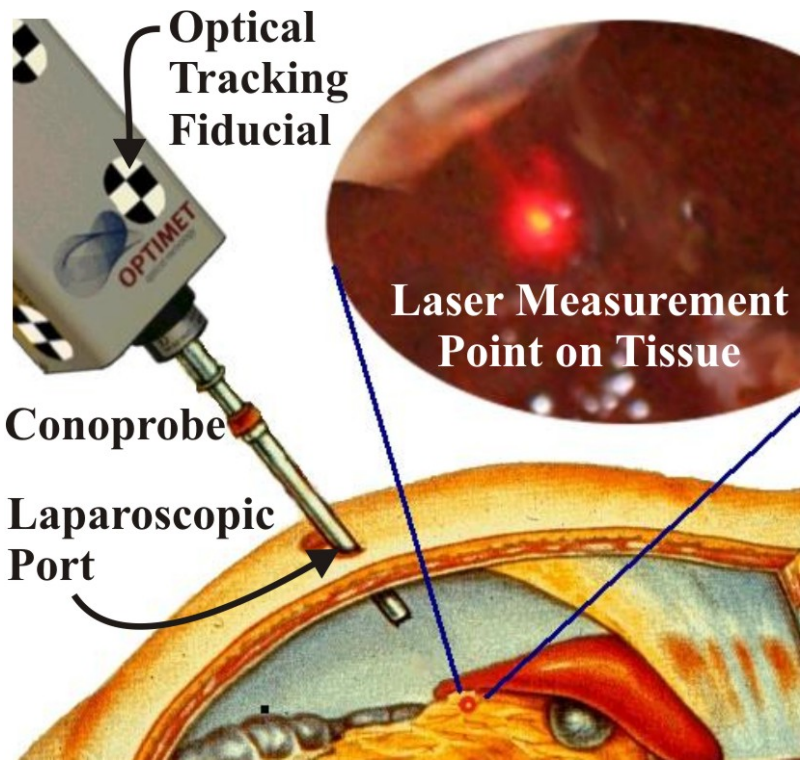

Figure 2. Conceptual drawing of organ surface scanning using conoscopic holography. The tracked conoscope returns distance measurements, which are converted to a point cloud that defines the shape of the tissue surface.

[1] Note that even if the return cone is encroached upon a small amount, the conoscope will still give a reasonable reading. Measurement accuracy degrades gracefully with increasing encroachment.

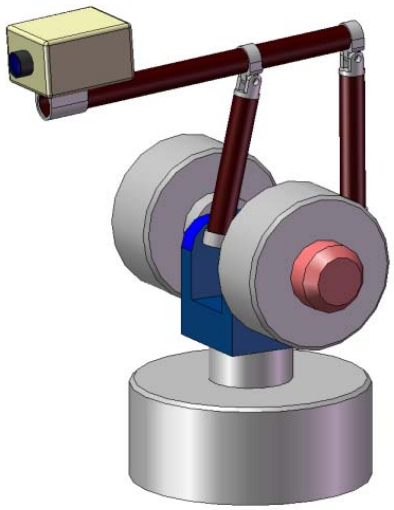

Figure 3. (Left) Virtual Environment Apparatus used as an encoding arm. (Right) CAD illustration of experimental sensing system

2.2 Optical Tracker

In the experiments that follow we used the MicronTracker 2 H3-60 (Claron Technology, Inc.). The H3-60 is a passive optical tracking system (shown at the right in Figure 7), which uses black and white checkerboard fiducials to identify and track objects in its field of view. The sensor head contains three 1280x960 pixel cameras whose images are processed using software supplied by the manufacturer to produce a coordinate frame transformation rigidly attached to the surface of the conoscope. The H3-60 has a roughly wedge shaped workspace extending from the sensor head, and targeting accuracy of a single vertex is specified to by the manufacturer at 0.20mm. The maximum sample rate is 15Hz, which in this paper also defines the maximum data capture rate in all the experiments. Note that the actual exposure of the CCD elements during image capture is approximately 1-3 ms (depending on light levels), and we compensated for this so that the conoscope measurements (which can be collected at higher frequencies) were recorded as nearly as possible in the middle of the imaging time to synchronize the two measurements.

2.3 Robotic Encoding Arm

Although not specifically used in the experiments that follow, our conoscope experimental setup also contains a mechanical robotic arm used for encoding. This is the Virtual Environment Apparatus [8] (see Figure 3). It performs the same task as the optical tracking system (namely resolving the motion of the conoscope) and will be used in future studies aimed at automatic conoscope manipulation and/or accuracy comparisons between mechanical and optical encoding.

3. BASELINE CONOSCOPE EXPERIMENTS

Two sets of experiments were preformed to explore the repeatability and accuracy of the conoscope when measuring distances to ex vivo and phantom tissues. These experiments establish the baseline capabilities of the conoscope, in order to provide context for the surface scanning results described in Section 4. We undertook these experiments because the published specifications of the conoscope, discussed in Section 2.1, assume non-biological surfaces such as metal or plastic, rather than red tissues which may absorb more of the red laser light. Note that there is no fundamental reason why conoscopic holography must use red lasers – other colors are possible. However, current commercial systems use red light, motivating these experiments. Our experimental setup for the experiments described in this section is shown in Figure 4, and consists of the conoscope, a linear slide, and the test sample. The axis of the linear slide is aligned with the conoscope laser, and provides relative tissue position accuracy of 0.01mm. Both the conoscope and the slide were firmly clamped to the working surface to ensure that they did not move relative to one another during the experiments.

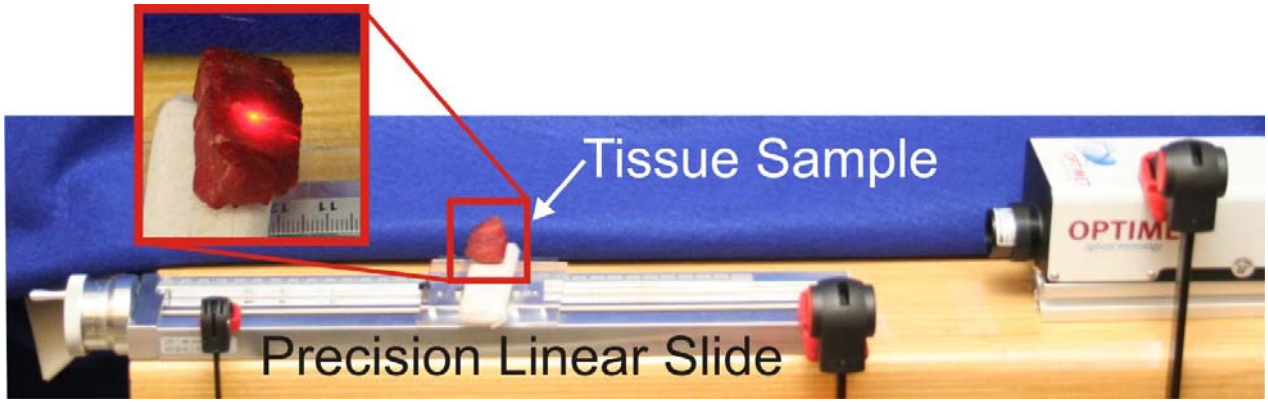

Figure 4. Baseline conoscope measurements were collected using a manually actuated precision linear slide. Tick marks on the actuation handle (visible at the left-hand end side of the slide above) can resolve 10 micrometers of linear sample motion. One full handle revolution produces 2mm of sample travel.

Tissue Types. In both of the following sets of experiments, three tissue types were considered. The "control sample" consisted of white paper attached to an aluminum block. The white surface provided a strong return signal with good signal to noise ratio, as reported by the conoscope. Ex vivo red tissue samples of bovine liver and bovine muscle were the other two tissue types used in these experiments. Proof of concept in bovine liver is particularly important, since previous surface scanning technologies have often been applied in image-guided liver surgery.

Conoscope Settings. The conoscope has two primary adjustable settings that can be modified to optimize performance for different surface types. These are the laser power level and sampling frequency of the CCD readings captured within the conoscope. These must be set to ensure adequate exposure of the CCD without saturation. Thus, for darker tissue types, one must increase power and/or reduce frequency. Through experimental tuning, we determined settings that yielded good results for our three tissue types, as shown in Table 1. We note, however, that this was not an exhaustive search, and it is possible that alternate settings may yield even better performance from the conoscope.

3.1 Repeatability Experiment

In order to determine the precision of conoscope measurements, we collected distance measurements at three discrete points in the conoscope's workspace: the beginning, middle, and end of the range. At each point, 10 measurements were recorded by momentarily interrupting and then reestablishing the conoscope's laser beam. This experiment was repeated with each of the three tissue types described above, and the standard deviations of the measurements are shown in Figure 5). We also experimented with topical surface preparation of the bovine liver sample (a surface dusting of talcum powder) as recommended by the manufacturer for less reflective surfaces. We did this not because of any deficiency in measurements made of untreated liver, but simply to assess the limits of the device to inform future application studies.

These results establish baseline error levels for the surface scanning experiments described in Section 4. They provide an indication of the relative portion of final measurement error induced by the sensor itself, and the portion that results from the use of optical tracking data to convert distance measurements into a point cloud. These experiments indicate that despite the color biological tissues, the conoscope produces measurements that are accurate enough for high-quality surface registration, since registration techniques are robust to some sensor noise.

Tissue Type	*White Paper*	*Bovine Muscle*	*Bovine Liver*	*Prep. Liver*
Conoscope Power Level	31.25%	62.5%	62.5%	62.5%
Conoscope Exposure Frequency	1000Hz	400Hz	100Hz	1000Hz

Table 1. Tuned conoscope power levels and acquisition rates for various tissue types. Power levels are listed as a percentage of the device's maximum output power. The prepared liver in the final column indicates an ex vivo liver sample dusted with talcum powder.

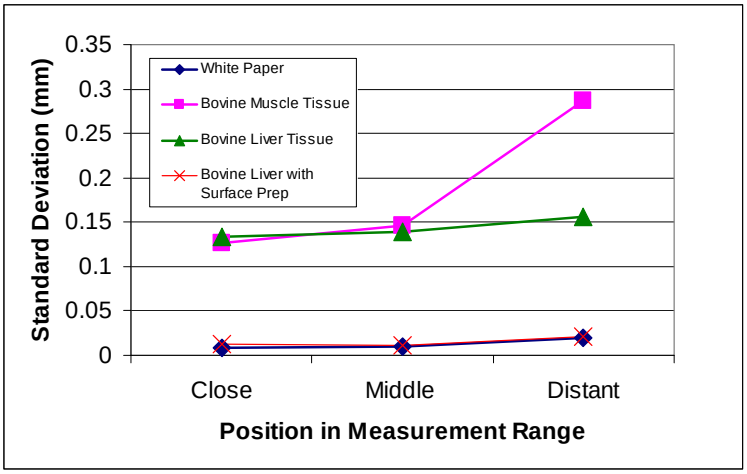

Figure 5. Standard deviations of repeated measurements taken with various tissue and control samples over the conoscope's measurement range. Each point represents the standard deviation of 10 measurements.

As evaluated experimentally in [1], commercial laser triangulation systems provide point clouds with approximately 1.3mm Fiducial Registration Error (FRE), and produce high-quality surface registrations. Note that directly comparing this FRE to the data presented in this section is not quite accurate, as the 1.3mm error also contains effects related to optical tracking. In section 4.4 we perform an experiment similar to that of [1] which enables a more direct comparison.

3.2 Accuracy Experiment

We performed a second set of experiments aimed at assessing accuracy over the conoscope's measurement range. To do this, we began by recording an initial position near the minimum end of the measurement range, which we defined as a reference position for subsequent measurements. The linear slide was then used to move the sample in increments of 10.00mm away from the conoscope until it reached the far end of the measurement range. For each increment, conoscope readings were used to compute distance traveled. The deviation of this distance increment from the actual increment of 10.00mm is plotted in Figure 6. This experiment shows that while liver yields the most variability, measurements do not drift over the range of the scanner.

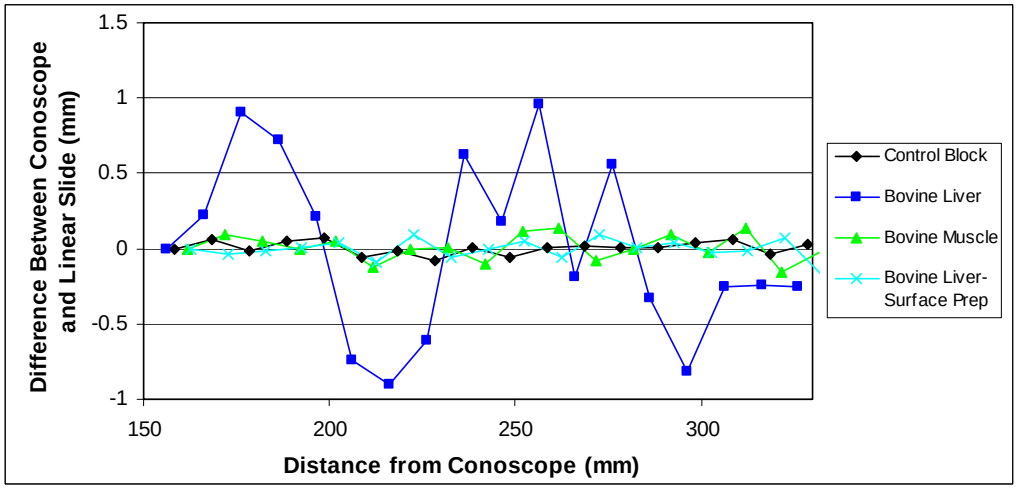

Figure 6. Experimental conoscope measurement error (vertical axis) vs. distance for biological tissues. Each data point above shows the difference from 10mm recorded by the conoscope when the sample was physically transported 10.00mm

Note that the specific values shown in Figure 6 will be highly dependent on the measurement increment, since the errors in measuring the points on each end of each measurement increment will be essentially fixed. Note also that again, a surface treatment of talcum powder is capable of making measurements of bovine liver nearly equivalent to those of the white paper of the control sample. The basic shape of the error in the untreated liver sample also appeared to be fairly repeatable, indicating that it may be possible to develop a calibration method to account for it, although this topic is left for future work.

4. SURFACE SCANNING EXPERIMENTS

The experimental setup for performing surface scans consisted of the conoscope with attached tracking fiducials, the optical tracker, various phantoms to be scanned, and a computer for recording synchronized data from the conoscope and tracker. For each measurement, the optical tracker reported the position and orientation of a point on the conoscope surface, and the conoscope reported a distance measurement. The two were synchronized using a timing signal originating in the conoscope that was activated at the beginning of each measurement.

During measurements, the conoscope was held approximately 1m in front of the optical tracker and 20-30cm from the phantom along the axis of the laser. The beam was manually scanned over the surface of the phantom. Both spherical and flat objects with a variety of surface properties were scanned in this way, and the data fit to the known shapes of the objects scanned. Before presenting the data, we describe the calibration and fitting processes necessary for accurately reconstructing the surface point cloud.

4.1 Calibration

First, the position of each sensed point on the surface was expressed in the world (optical tracker) frame as,

$$ {}^{world}p_{sensed} = {}^{world}T_m \, {}^{m}T_c \, {}^{c}p_{sensed}, \tag{1} $$

where *c* denotes the conoscope lens frame and *m* denotes the fiducial marker frame. Here ${}^{c}p_{sensed}$ has zero y and z components and the conoscope reading as its x component. The transformation ${}^{world}T_m$ is given directly by the optical tracking system. The transformation between the conoscope measurement frame (located at its lens) and the fiducial marker frame on its surface, ${}^{m}T_c$, is unknown and must be determined by calibration.

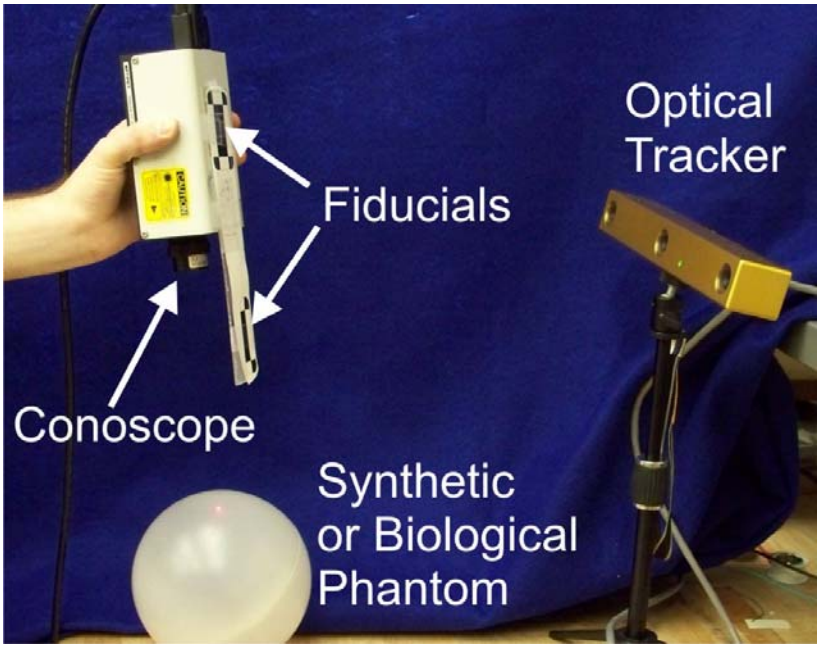

Figure 7. Experimental setup for surface scanning using the tracked conoscope.

In contrast to rigid surgical tools where one might apply a pivot calibration, the distance to the point of interest here has no rigid physical structure attached to it. Thus we calibrated using variable measurements along its axis returned by the conoscope. In this case, one might also consider applying a solution to the "Hand-Eye" calibration problem (e.g. the dual quaternion formulation of [11]), but in our case a simpler calibration procedure is possible, since we know that sensed measurements will always lie along a single axis in the sensor (conoscope lens) frame.

We performed this calibration by aiming the conoscope laser at a second fiducial marker that was not attached to the conoscope, the position of which $({}^{world}P_n)$ was sensed by the optical tracking system. We repeated this for several different conoscope poses. Then, parametrizing the rotation using X-Y-Z Euler angles, we applied MATLAB's `fminsearch` to minimize,

$$e = \sum_i a_i^T a_i \text{ , where } a_i = {}^{world}p_n - {}^{world}T_{m,i}\,{}^{m}T_c\,{}^{c}p_{sensed,i}$$

over the Euler angles and translation that compose the unknown transformation. The sum over $i \in \{1...n\}$ accounts for each of the *n* conoscope pose measurements made above.

4.2 Registration Algorithm

We conducted experiments with two parametric surfaces, a plane and a sphere. The algorithm for registering the known shape to the data was identical in both cases, except for the objective function. In both cases, we minimized the surface parameters over the distance between measured data and the known surface shape using MATLAB's `fminsearch`. For the plane $ax + by + cz + d = 0$, we minimized the sum of the square of distances between the plane and each point,

$$e_{plane} = \sum_i \left(ax_i + by_i + cz_i + d\right)^2 ,$$

over the parameters of the plane, *a*, *b*, *c*, and *d*.

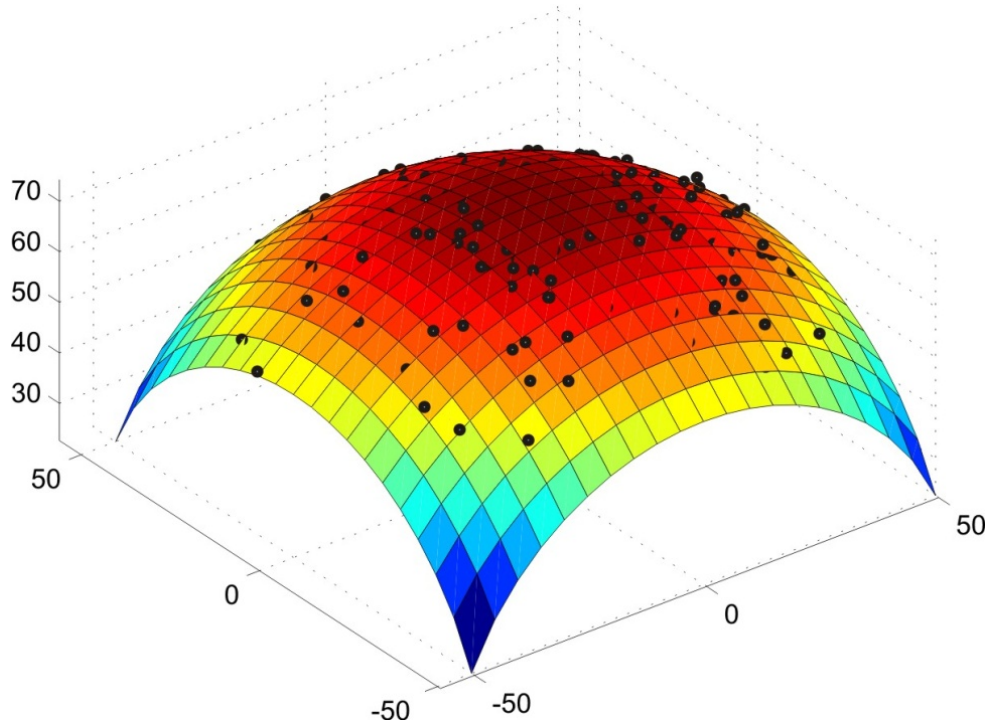

Figure 8. When used to scan a plastic sphere, the conoscope returns a point cloud (black dots above) which can be used to align preoperative image information (here represented by the spherical surface) with this "intraoperative" point cloud.

For the sphere $(x-x_c)^2+(y-y_c)^2+(z-z_c)^2=r^2$, we minimized the sum of the square of the radial distances between the sphere and each point, namely,

$$e_{sphere}=\sum_i\left((x_i-x_c)^2+(y_i-y_c)^2+(z_i-z_c)^2-r^2\right)^2,$$

over the sphere parameters x_c, y_c, z_c, and r.

4.3 Parametric Surface Scans

Using the calibration and registration procedures outlined above, we scanned and fit two planes and two spheres. A control plane was created by attaching a piece of white paper to a flat metal surface. A liver "plane" was created by laying a 5.4mm think slice of bovine liver flat on a piece of metal. While this did not create a perfectly flat liver surface, it did create one that was as nearly flat as possible. We also scanned a semi-translucent, polypropylene plastic sphere, as well as a "liver sphere". The liver sphere created in a similar manner as with the flat liver phantom by draping the same 5.4mm slice of liver over the plastic sphere. We collected point clouds with the conoscopic holography system for each of these surfaces, and as described in the previous section, fitted the clouds to their corresponding parametric surfaces. The results of these experiments are summarized on Table 2. Figure 8 shows the data returned from the conoscope scan of the plastic sphere point cloud on top of a sector of a sphere that has been fitted to the data.

Object	***Paper Plane***	***Liver Plane***	***Plastic Sphere***	***Liver Sphere***
Number of points	800	400	400	400
Surface	White Paper	Liver	Semi-Translucent	Liver
Actual Radius	N/A	N/A	75.0mm	80.4mm
Fit Radius	N/A	N/A	74.3mm	81.0mm
Standard Deviation	0.24mm	1.22mm	0.47mm	0.61mm

Table 2. This table describes the four parametric surfaces scanned, and lists the fitted values, which closely approximate the actual parameter values. Standard deviations provide a measure of the quality of fit between the data and the surface.

4.4 Phantom and Ex Vivo Liver Scans

A final experiment was conducted to assess the conoscope's ability to scan and reconstruct a general surface that is representative of human liver. To create this surface, we placed four fiducial markers (pins with large plastic heads) into a dark red cast rubber sample shaped as a human liver. The four pins serve as fiducials for registering multiple scans. We then scanned the sample surface with the conoscope, separately scanning the fiducials. To collect a second data set, we then rotated the metal plate holding the sample by approximately 90 degrees, and scanned the surface and fiducials again using the same procedure.

In order to compare the two data sets, we rigidly registered them using Arun's method [12] on the positions of the four fiducal pins in each. This resulted in a FRE of 0.94mm. Note that this level of FRE is similar to the approximately 1.3mm reported in literature for laser triangulation systems [1], which suggests that conoscopic holography is a feasible technolgy for registering preoperative images to interaoperative surface contours described by point clouds. To visualize the quality of fit of the two registered point clouds, the two clouds were triangularized (using an algorithm based on the 2.5D Delaunay criterion) and then plotted together (see Figure 9).

Ex vivo liver scan visualization. To photographically visualize a surface scan of ex vivo liver, we piled bovine liver on a metal sheet until it had a contoured surface that qualitatively resembled in vivo human liver. Figure 10 shows the liver sample together with a scanned point cloud describing its surface. The figure was generated by plotting the point cloud data in MATLAB, and moving the MATLAB camera viewpoint as nearly as possible to the perspective from which the image was taken (near the origin of the world frame). This placed the point cloud at the correct orientation. To match it to the image, all that was necessary was to manually scale and rotate (but not warp or otherwise deform) the point cloud plot until the four fiducial points in it matched those in photograph of the liver as nearly as possible.

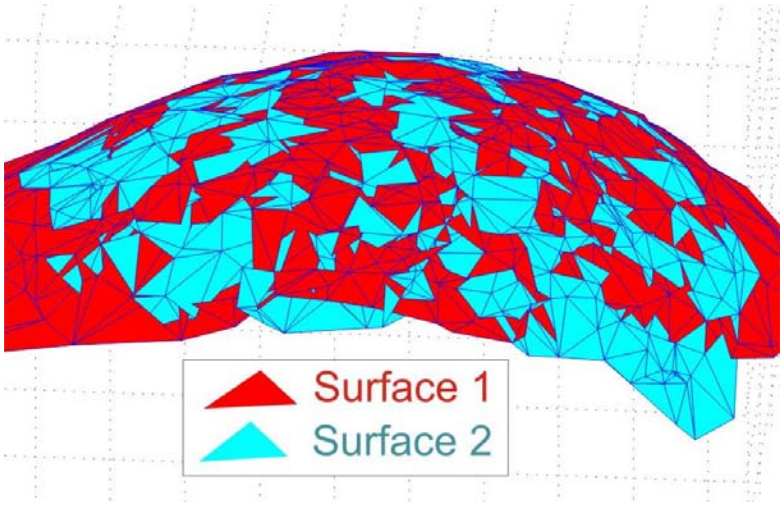

Figure 9. A visualization of two registered surface point clouds converted to surfaces using Delaunay triangulation. These two point clouds describe the surface of a red rubber phantom cast in the shape of a human liver, and were registered using fiducial markers.

5. CONCLUSION

We have described in this paper our experiments exploring the feasibility of using conoscopic holography as a laparoscopic surface scanning technique. The promise of conoscopic holography is the ability to scan through a laparoscopic port without requiring wide exposure of the abdomen or other cavity. The facts that conoscopic holography is a proven technique used for high precision distance measurements, is readily available in off-the-shelf, inexpensive packages, and can deliver high-quality distance measurements to biological tissues make it a compelling candidate for laparoscopic surface scanning. As has been demonstrated with previous laser triangulation and touch-probe systems, surface scan data can enable the information in preoperative images to be registered and used more directly in surgery, which has the potential to increase accuracy and safety in needle placement and other procedures. Examples of ways this information might be used include augmented visual displays to assist the physician (e.g. image overlay [9]), or direct use in a robotic system to accurately position a tool to a desired subsurface location (see e.g. [10]). The experiments we have presented here indicate that conoscopic holography can provide adequate accuracy and precision for surface scanning, even in red biological tissues. This work motivates future studies to more fully vet conoscopic holography in in vivo clinical settings when tissues are perfused. However, the preliminary results presented here in ex vivo tissues are highly encouraging. They support the notion that conoscopic holography has the potential to become a useful tool in the ongoing effort to provide doctors with accurate, timely, and integrated information to inform intrasurgical decision making.

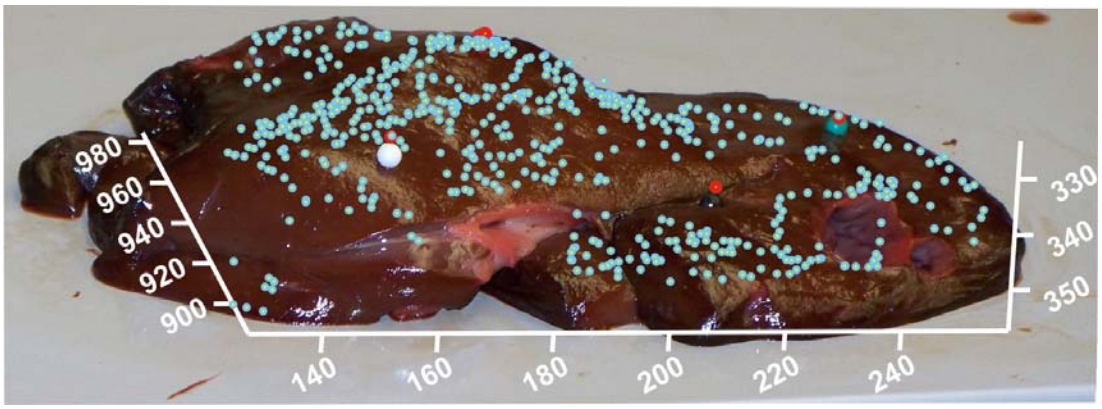

Figure 9. Points representing a surface scan of a bovine liver sample. Axis markings are in millimeters.

ACKNOWLEDGEMENTS

The authors wish to acknowledge Robert Galloway for assistance with the initial problem definition as well as implementation advice. Panadda Marayong, Henry Lin, Prashanth Dumpuri assisted with software for registration and Steve Mate with Co-Efficient, Inc. who provided assistance and software for the conoscope sensor. Special thanks to Michael Doherty and Optimet, Inc. for the loan of the Conoprobe sensor head. Funding for this work was provided by Vanderbilt University.

REFERENCES

[1] Miga, M. I., Sinha, T. K., Cash, D. M., Galloway, R. L., and Weil, R. J., "Cortical surface registration for image-guided neurosurgery using laser-range scanning", *IEEE Transactions on Medical Imaging*, 22(8), 973-985, (2003).

[2] Grimson, W.E.L., Ettinger, G. J., White, S. J. , Perez, T.L., Wells, W. M., Kikinis, R., "An automatic registration method for frameless stereotaxy, image guided surgery, and enhanced reality visualization", *IEEE Transactions on Medical Imaging*, 12(2), (1996).

[3] Herline, A.J., Herring, J.L., Stefansic, J.D., Chapman, W.C., Galloway, R.L., Dawant, B.M., "Surface registration for use in interactive, image-guided liver surgery," *Medical Imaging Computation and Computer-Assisted Intervention*, 892-899, (1999).

[4] SurgiSight system, Pathfinder Therapeutics, Inc. Nashville, TN.

[5] Cash, D.M., Sinha, T.K., Chapman, W.C., Dawant, B.M., Galloway, R.L., Miga, M.I., "Incorporation of a laser range scanner into image-guided liver surgery: Surface acquisition, registration, and tracking" *Medical Physics*, 30(7), 1671-1682, (2003).

[6] Sirat, G., Psaltis, D. "Conoscopic holography," *Optics Letters*, 10(1), (1985).

[7] Sirat, G., Paz, F., Agronik, G., Wilner, K., "Conoscopic Systems and Conoscopic Holography", *Optimet*, POB 45021, Jerusalem 91450, Israel.

[8] Kilchenman O'Malley, M., and Goldfarb, M., "Comparison of Human Haptic Performance in Real and Simulated Environments" *Proceedings of the IEEE 10th International Symposium on Haptic Interfaces for Virtual Environment and Teleoperator Systems*, 10-17, (2002).

[9] Fischer, G.S., Deguet, A., Csoma, C., Taylor, R.H., Fayad, L.M., Carrino, J.A., Zinreich, S.J., Fichtinger, G., "MRI Image Overlay: Application to Arthrography Needle Insertion," *Journal of Computer Assisted Surger*, 12(1), 2-14, (2007).

[10] Boctor, E.M., Choti, M.A., Burdette, E.C., and Webster III, R. J., "Three-Dimensional Ultrasound-Guided Robotic Needle Placement: An Experimental Evaluation," *International Journal of Medical Robotics and Computer Assisted Surgery*. 4(2), 180-191, (2008).

[11] Daniilidis, K., "Eye-Hand Calibration Using Dual Quaternions" International Journal of Robotics Research, 18(3), 286-298, (1999).

[12] Arun, K.S., Huang, T.S., Blostein S.D, "Least-squares fitting of two 3-D point sets" *IEEE Transactions on Pattern Analysis and Machine Intelligence*, 9(5), 698-700, (1987).